



# LUND UNIVERSITY

## Highly efficient generation of induced neurons from human fibroblasts that survive transplantation into the adult rat brain.

Pereira, Maria J M; Pfisterer, Ulrich; Rylander, Daniella; Torper, Olof; Lau, Shong; Lundblad, Martin; Grealish, Shane; Parmar, Malin

*Published in:*  
Scientific Reports

*DOI:*  
[10.1038/srep06330](https://doi.org/10.1038/srep06330)

2014

[Link to publication](#)

### *Citation for published version (APA):*

Pereira, M. J. M., Pfisterer, U., Rylander, D., Torper, O., Lau, S., Lundblad, M., Grealish, S., & Parmar, M. (2014). Highly efficient generation of induced neurons from human fibroblasts that survive transplantation into the adult rat brain. *Scientific Reports*, 4, Article 6330. <https://doi.org/10.1038/srep06330>

*Total number of authors:*  
8

### **General rights**

Unless other specific re-use rights are stated the following general rights apply:

Copyright and moral rights for the publications made accessible in the public portal are retained by the authors and/or other copyright owners and it is a condition of accessing publications that users recognise and abide by the legal requirements associated with these rights.

- Users may download and print one copy of any publication from the public portal for the purpose of private study or research.
- You may not further distribute the material or use it for any profit-making activity or commercial gain
- You may freely distribute the URL identifying the publication in the public portal

Read more about Creative commons licenses: <https://creativecommons.org/licenses/>

### **Take down policy**

If you believe that this document breaches copyright please contact us providing details, and we will remove access to the work immediately and investigate your claim.

LUND UNIVERSITY

PO Box 117  
221 00 Lund  
+46 46-222 00 00





## OPEN

SUBJECT AREAS:  
REPROGRAMMINGREGENERATION AND REPAIR IN  
THE NERVOUS SYSTEMReceived  
15 May 2014Accepted  
19 August 2014Published  
11 September 2014Correspondence and  
requests for materials  
should be addressed to  
M.P. (malin.parmar@  
med.lu.se)

# Highly efficient generation of induced neurons from human fibroblasts that survive transplantation into the adult rat brain

Maria Pereira, Ulrich Pfisterer, Daniella Rylander, Olof Torper, Shong Lau, Martin Lundblad, Shane Grealish &amp; Malin Parmar

Department of Experimental Medical Science, Wallenberg Neuroscience Center and Lund Stem Cell Center, Lund University, 221 84 Lund, Sweden.

Induced neurons (iNs) offer a novel source of human neurons that can be explored for applications of disease modelling, diagnostics, drug screening and cell replacement therapy. Here we present a protocol for highly efficient generation of functional iNs from fetal human fibroblasts, and also demonstrate the ability of these converted human iNs (hiNs) to survive transplantation and maintain their phenotype in the adult rat brain. The protocol encompasses a delay in transgene activation after viral transduction that resulted in a significant increase in conversion efficiency. Combining this approach with treatment of small molecules that inhibit SMAD signalling and activate WNT signalling provides a further increase in the conversion efficiency and neuronal purity, resulting in a protocol that provides a highly efficient method for the generation of large numbers of functional and transplantable iNs from human fibroblasts without the use of a selection step. When transplanting the converted neurons from different stages of *in vitro* culture into the brain of adult rats, we observed robust survival and maintenance of neuronal identity four weeks post-transplantation. Interestingly, the positive effect of small molecule treatment observed *in vitro* did not result in a higher yield of iNs surviving transplantation.

Cellular reprogramming, where somatic cells are turned into stem cells or other somatic cell types, has opened up new and previously unconsidered possibilities to obtain patient- and disease-specific neurons on demand<sup>1</sup>. Such neurons can be obtained via generation of induced pluripotent stem (iPS) cells<sup>2</sup>, where fibroblasts are reprogrammed into pluripotent stem cells that subsequently can be differentiated into any cell lineage, including neurons; or by expression of specific sets of neural conversion genes resulting in direct reprogramming into induced neurons (iNs) or induced neural precursor cells (iNPCs) *in vitro*<sup>3,4</sup>.

Subtype specific iNs can be obtained from human fibroblasts<sup>5–8</sup>, and thus represent a supply of human neurons that can be generated on demand and used in biomedical applications and for disease modelling. For example, induced neurons obtained via direct conversion of fibroblasts from a patient with Alzheimer's disease or from transgenic mice with autism-associated neuroligin-3 mutation have been shown to mimic pathologic conditions and abnormal neuronal phenotype<sup>9,10</sup>, substantiating their predicted use as disease models for neurological disorders as a quicker and simpler alternative to iPS cells for this purpose.

Direct neural conversion is also a very promising technology to develop for use in cell replacement therapies since iNs are not formed via a proliferative cell intermediate<sup>3,11</sup>, and thus may represent a safer source of clinically relevant transplantable neurons in the future. However, in order to fully realize the potential of hiNs in regenerative medicine, much work is required to increase conversion efficiency and to analyse survival and maturation of hiNs after transplantation, as well as to develop clinically compatible reprogramming vectors<sup>12,13</sup>.

Here we report a highly efficient protocol for direct neural conversion that involves delayed transgene activation and improved culture conditions in combination with the addition of small molecules (SMs) that inhibit SMAD signalling and activate canonical WNT signalling<sup>14</sup>. This protocol results in at least a 10-fold improvement of conversion efficiency compared to previous reports<sup>5–7,15,16</sup>, and therefore provides a method for highly efficient generation of iNs from human fibroblasts without the need for a drug selection step. Furthermore, we provide the first evidence that hiNs survive and maintain their phenotype after transplantation into the adult rat brain, when

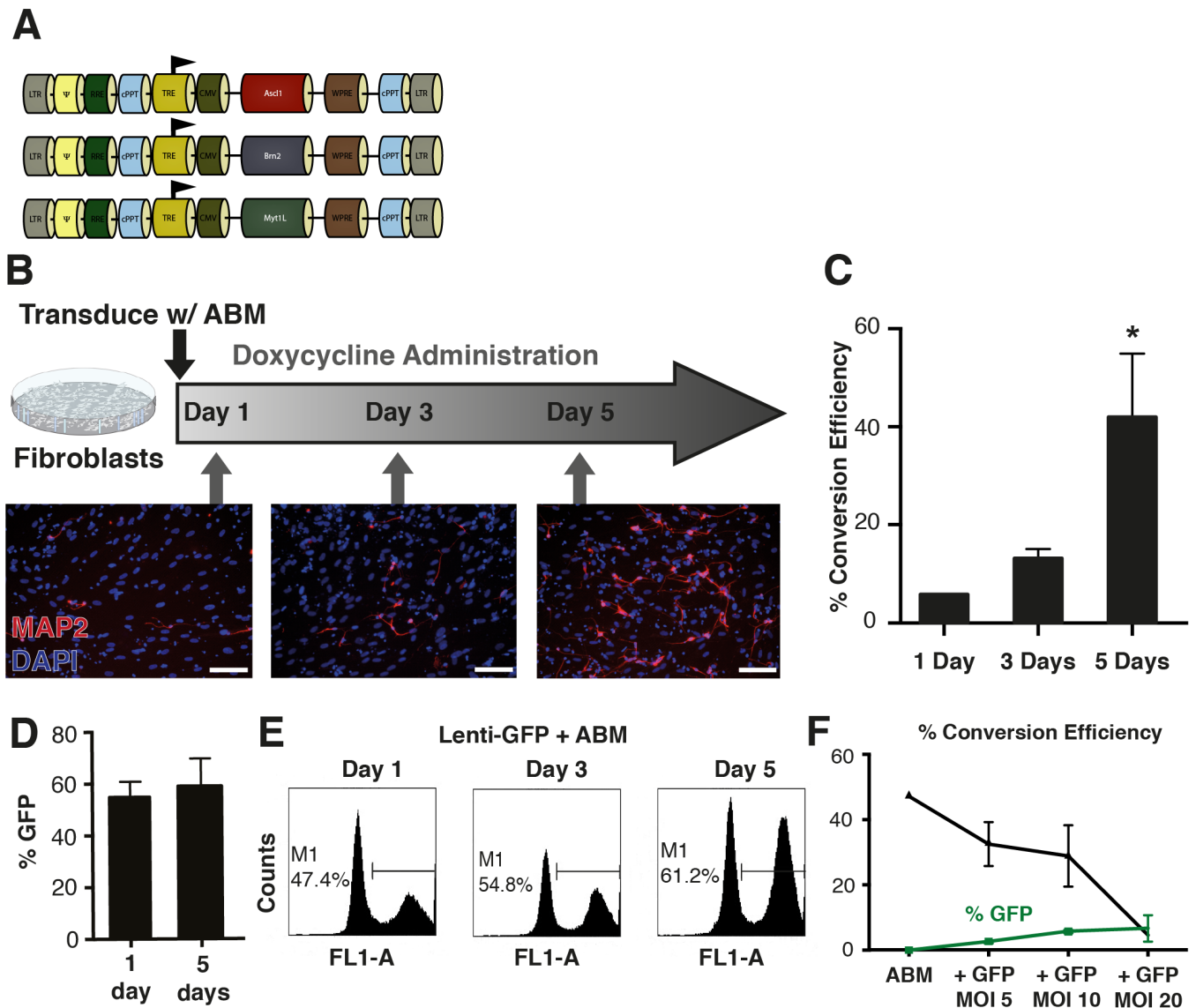


**Figure 1 | Delay in transgene activation improves conversion efficiency *in vitro*.** (A) Map of constructs used for conversion. (B) Overview of experiment and fluorescence microscopy pictures show that delaying the activation of ABM *in vitro* results in increasing yields of MAP2<sup>+</sup> hiNs. (C) Doxycycline administration 5 days after transduction significantly increases conversion efficiency, assessed 15 days after transgene activation and based on MAP2 expression of the hiN cells, ( $n = 3$ ),  $* = p < 0.05$ , 5 days-delay significant compared to 1 day-delay [Group,  $F_{(2,6)} = 6.58$ ,  $p < 0.05$ , confirmed using a Tukey *post hoc*]. (D) FACS analysis of GFP<sup>+</sup> cells at 1 and 5 days post-transgene activation did not reveal a difference in the proportion of transduced cells. (E) FACS analysis of GFP level 1, 3 and 5 days after transduction of fibroblasts, revealed that there is an increase in the number of cells expressing a higher level of the transgene, here assessed by GFP expression, when the interval of delay increases. (F) The use of a GFP-expressing virus to transduce human fibroblasts, 5 days after delivering the reprogramming genes ABM, at the time of transgene activation, led to a decrease in conversion efficiency (%) in a dose-dependent manner when increasing MOIs (5, 10 and 20) were used. Scale bars: B = 100  $\mu$ m.

transplanted 5 and 10 days after initiation of conversion. In contrast to the *in vitro* studies, we did not observe an effect on graft survival or content, when hiNs had been exposed to small molecules in culture prior to transplantation.

## Results

In order to test if varying the time between viral transduction and transgene activation affects conversion efficiency, human fetal fibroblasts were plated and transduced with the same doxycycline-regulated viral vector mix containing Ascl1, Brn2a and Myt1l (ABM, Fig. 1A) previously shown to efficiently convert mouse and human fibroblasts into functional neurons<sup>3,5</sup>. Doxycycline was added to culture medium to activate the reprogramming genes 1, 3, 5 and 12 days after transduction, during which time the cells continued to proliferate. Delays longer than 5 days results in extensive prolifera-

tion and overgrowth of the fibroblasts that started to de-attach making further analysis impossible. However, in cultures with 1, 3 and 5 days delay of administration, converted neurons could be detected by MAP2 staining 15 days after conversion (Fig. 1B). When quantifying the MAP2-expressing cells, we found that when delaying transgene activation, the conversion efficiency, as determined by the number of neurons formed divided by the number of fibroblasts plated<sup>3</sup>, was increased from  $5.77 \pm 0.18\%$  to  $42.20 \pm 12.86\%$  (Fig. 1C). This increase in conversion efficiency can largely be attributed to proliferation of the transduced fibroblasts simply resulting in a higher number of cells expressing the reprogramming factors. However, the proportion of transduced cells remained unchanged (Fig. 1D), and yet the neuronal purity, as determined by the number of iNs expressed as a percentage of the total cell number, based on DAPI counts<sup>14</sup>, 15 days after conversion increased from  $0.97 \pm 0.41$  to  $3.42$





$\pm 0.67\%$ . This suggests that additional parameters contribute to a higher conversion rate after delayed transgene activation. We postulated that factors such as the level of transgene expression, as well as the condition of cells at initiation of conversion, could contribute to the increased conversion efficiency. When experimentally addressing this, we found that the level of transgene expression increases with a delayed transgene activation as assessed using a GFP-reporter (Fig. 1E). To estimate the effect of viral infection following an immediate initiation of conversion, as used in previous protocols with no delay of transgene activation, we performed an experiment where at 5 days after delivering the reprogramming genes (at the time of transgene activation in new protocol) the cells were further transduced with a GFP-virus. We found that viral infection at the time of transgene activation leads to a decrease in conversion efficiency in a dose-dependent manner (Fig. 1F and Supplementary Fig. S1). In summary, these data suggest that a higher transgene expression in addition to a sufficient recovery of the targeted cells after viral transduction is likely to contribute to the increased conversion observed.

It was recently reported that addition of SMs, which inhibit SMAD signalling as well as a GSK3 $\beta$  inhibitor that activates canonical WNT signalling, significantly increases the conversion efficiency of human fibroblasts<sup>14</sup>. We tried this new SM treatment separately and in combination with our new approach of delaying doxycycline administration when converting fibroblasts using ABM (Fig. 2B–D). We utilised an automated and unbiased system (Cellomics array scan, Thermo Scientific) for performing quantifications of conversion efficiency and neuronal purity based on MAP2 expression of converted cells 15 and 22 days after transgene activation. The number of iN cells remained stable between 15 and 21–23 days and all conditions showed an increase of conversion efficiency as well as purity over baseline (Fig. 2C,D). The combined treatment of delayed doxycycline transgene activation and SM treatment resulted in the highest conversion efficiency of  $121.7 \pm 12.4\%$  (Fig. 2C) and a purity over 20% (Fig. 2D). To provide another assessment of the conversion efficacy that is based on number of targeted cells, we cloned a bicistronic construct linking the gene *Ascl1* (that encodes for MASH1 protein) to a GFP reporter via an internal ribosome entry site (*Ascl1*-IRES-GFP, Fig. 2A). This construct resulted in high overlap between MASH1 and GFP when cells are exposed to doxycycline (Fig. 2E, E', E'', F), and no expression of MASH1 or GFP in the absence of doxycycline (Supplementary Fig. S2). A low level of conversion was observed when cells were transduced with *Ascl1*-IRES-GFP construct, however when combined with transduction of the other conversion factors *Brn2a* and *Myt1l* a high number of neurons expressing GFP were generated (Fig. 2G–G''). Given that GFP and MASH1 is co-expressed in more than 80% of the cells, and that we have a high co-transduction of cells in culture when using several lentiviruses, the co-expression of GFP and MAP2 provides an approximation of the ability of the targeted cells to convert into neurons. Using this method for assessing conversion, we estimate that  $46 \pm 13\%$  and  $61 \pm 4\%$  of the targeted cells converted into MAP2-expressing iNs without and with SMs respectively, when using *Ascl1*-IRES-GFP, *Brn2a* and *Myt1l* for conversion.

In summary, by using our new protocol encompassing delay in transgene activation combined with SM treatment, we can obtain a high number of hiNs co-expressing the neuronal markers MAP2 and Beta-III-tubulin (Fig. 2H, H'), in the absence of fibroblast markers such as Collagen (Fig. 2I), with very high efficiency and without incorporating a selection step as used in previous reports with comparable efficiencies<sup>14,17</sup>.

When analysing the morphological complexity of the hiNs using Cellomics (Fig. 3A, A', A''), we could not detect a difference in the number of processes per neuron (Fig. 3B, B'), and only subtle effects on total neurite length per neuron (Fig. 3C, C'). This suggests that SMs greatly increase the efficiency of hiN conversion, but do not affect the overall morphological complexity of the hiNs generated.

With a protocol that robustly results in a high number of hiNs, we next investigated the functional properties of the obtained cells. Electrophysiological recordings at 48–50 days post conversion confirmed that the hiNs exhibited electrophysiological properties characteristic of functional neurons. The majority of cells displayed inward and outward currents ( $n = 12/14$  cells) indicative of inward sodium and delayed-rectifier potassium currents (Fig. 3D). Moreover, 78% of the recorded hiNs were able to fire action potentials after current injections ( $n = 11/14$  cells, Fig. 3E). When ABM converted iNs were co-cultured with astrocytes for 90 days, they developed post-synaptic currents indicative of them sending and receiving synaptic input (Fig. 3F). In summary, hiNs generated using delayed transgene activation in combination with SM treatment exhibited electrophysiological properties characteristic of neurons, that are similar to previous reports of hiNs<sup>14,15</sup>.

In previous reports, where neural conversion has been performed using ABM or in the presence of SMs, GABAergic and glutamatergic neurons have been the predominant subtype generated<sup>3,5,14,15</sup>. We performed immunocytochemical analysis to analyse the subtype of neurons being formed under our culture conditions. We could confirm the presence of GABAergic neurons (Fig. 4A) and the near absence of neurons expressing TH (dopaminergic neurons), 5-HT (serotonergic neurons) and ChAT (cholinergic neurons) using immunocytochemistry. In conditions without small molecules,  $29.5 \pm 0.4\%$  of the hiNs expressed GABA and this proportion was increased to  $39.5 \pm 2.1\%$  when small molecules were added. Next we performed qPCR analysis of the hiNs purified using FACS, based on their expression of human-specific neural cell adhesion molecule (hNCAM) (Fig. 4B), and confirmed the presence of inhibitory and excitatory neurons by the expression *GAD67* and *vGLUT1*, (Fig. 4C). The hiNs also expressed high levels of *ISL1* when cells are exposed to SMs, but only very little *DARPP32* and no ChAT, suggesting that at least a proportion of the GABAergic neurons appearing after exposure to SM were of an immature striatal phenotype (Fig. 4C). We could also detect increased levels of the NMDA receptor *NR2A* after exposure to SMs (Fig. 4C).

The ability to generate dopamine neurons via direct conversion is of particular interest in the field of cell replacement therapy, since these are the neurons that are affected in Parkinson's disease. Thus, we tested our new protocol for iN conversion with the addition of four dopamine neuron fate determinants, *Lmx1a*, *Lmx1b*, *FoxA2* and *Otx2*, previously identified to yield a high number of TH-expressing iNs<sup>18</sup>. Using these conversion factors with our new protocol encompassing delayed transgene activation and delivery of SMs, we found the neural conversion efficiency and purity remained at the same high level (Fig. 4D–F), while the mean number of TH-expressing neurons increased from  $96.3 \pm 55.6$  to  $503.4 \pm 205.5$ . To test the functionality of the DA-hiNs, we developed a setup for *in vitro* electrochemical monitoring of dopamine release from cultured cells (see Materials and Methods for details). The cells were placed in dopamine-containing buffer ( $10$ – $15 \mu\text{M}$  DA) for 60 s and 120 s. After dopamine flow was terminated, the cells were depolarized with KCl, and we could confirm that the cells converted using ABM plus the four DA determinants released dopamine upon depolarization whereas no dopamine release was registered in the ABM only cells (Fig. 4G–I). This demonstrates that the cells converted with ABM and DA fate determinants can take up and load dopamine into vesicles, and also release dopamine upon depolarization.

We next analysed the potential of the resulting hiNs converted using ABM plus the four DA determinants to survive transplantation and mature in the adult rodent brain. To determine the optimal maturation state of cells for transplantation as well as the effect of SM treatment, we transplanted 5 groups of hiNs obtained under different conditions into the striatum of adult rats kept under daily immunosuppression using ciclosporin. Cells generated under the following conditions were transplanted: hiNs kept in culture for 4

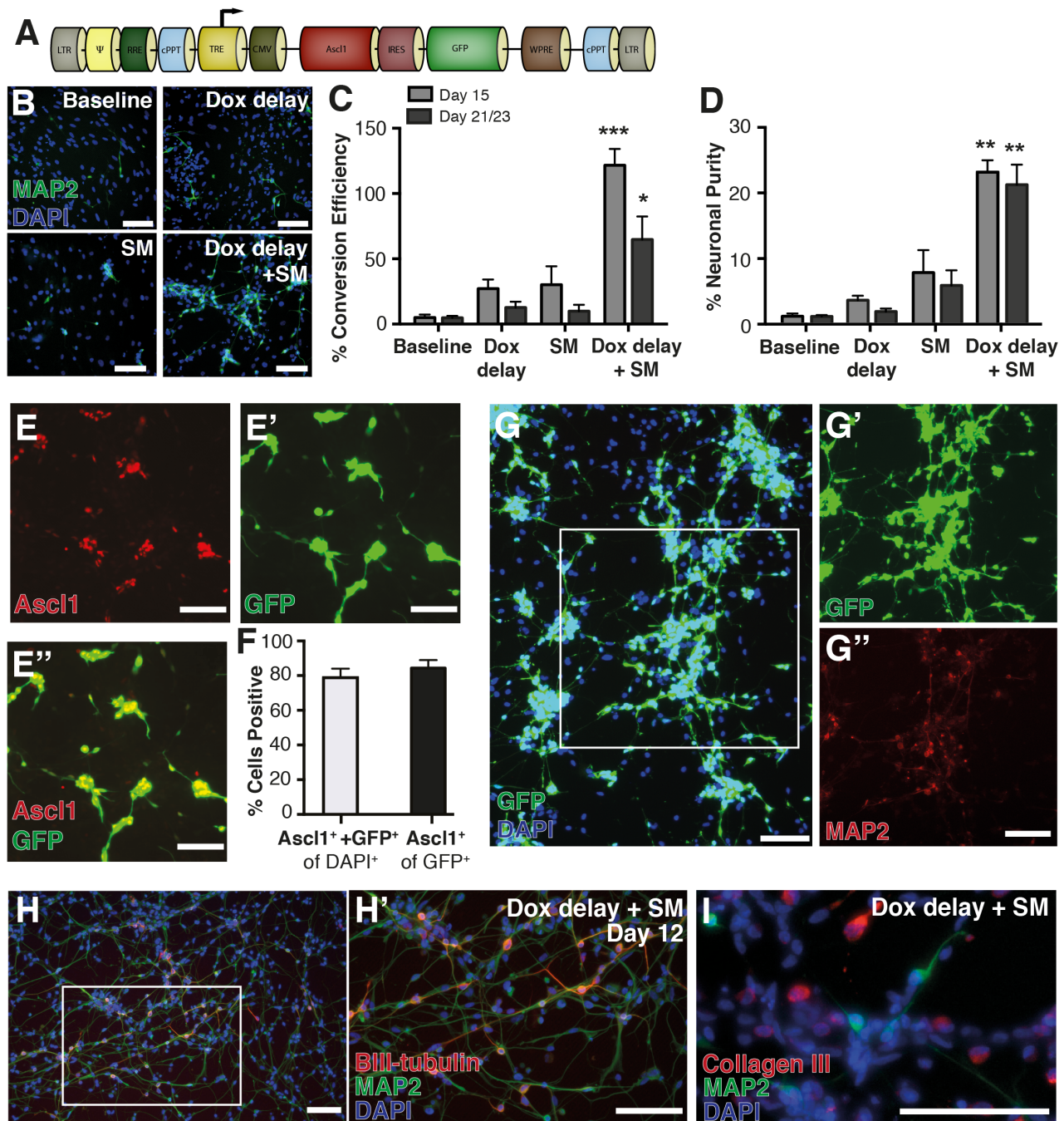


**Figure 2 | Combination of delayed transgene activation and small molecules have an accumulative effect.** (A) Map of bicistronic Ascl1-IRES-GFP construct. (B) Immunofluorescent staining for MAP2 of hiNs, 15 days after transgene activation, shows an increased yield of MAP2<sup>+</sup> hiNs generated using the combinatorial protocol of doxycycline delay and small molecules (Dox delay + SM), in comparison with the other conditions. (C) Conversion efficiency of hiNs converted with ABM 15 days after transgene activation (n = 3), \*\*\* = p < 0.0001, Dox delay + SM significant compared to Baseline, Dox delay and SM [Group,  $F_{(3,8)} = 26.25$ , p < 0.001, confirmed using a Tukey *post hoc*] and 21/23 days after transgene activation (n = 3), \* = p < 0.05, Dox delay + SM significant compared to Baseline, Dox delay and SM [Group,  $F_{(3,8)} = 8.84$ , p < 0.001, confirmed using a Tukey *post hoc*]. When comparing the conversion efficiency obtained for each individual condition, between time points, no differences were found (n = 3), p = n.s. for all the performed comparisons. (D) Neuronal purity of hiNs converted with ABM 15 days after transgene activation (n = 3), \*\* = p < 0.001, Dox delay + SM significant compared to Baseline, Dox delay and SM, [Group,  $F_{(3,8)} = 24.66$ , p < 0.0001, confirmed using a Tukey *post hoc*], and 21/23 days after transgene activation (n = 3), \*\* = p < 0.001, Dox delay + SM significant compared to Baseline, Dox delay and SM, [Group,  $F_{(3,8)} = 23.58$ , p < 0.0001, confirmed using a Tukey *post hoc*]. When comparing the conversion efficiency obtained for each individual condition, between time points, no differences were found (n = 3), p = n.s. for all the performed comparisons. (E-E'') Fluorescence microscopy image and quantifications show a high overlap between MASH1 and GFP from the Ascl1-IRES-GFP construct. (G-G'') Cells converted with Ascl1-IRES-GFP and BM result in a high overlap of MAP2<sup>+</sup> and GFP 16 days after initiation of transgene expression. (H and H') Fluorescence microscopy pictures show co-labelling of MAP2<sup>+</sup> and BIII-tubulin<sup>+</sup> hiNs converted with ABM using the new conversion protocol (Dox delay + SM), 12 days after transgene activation. (I) MAP2<sup>+</sup> hiN cells in culture do not co-express Collagen III, 15 days after transgene activation. Scale bars: (B), (E-E''), (G, G'), (H, H') and (I) = 100 μm.



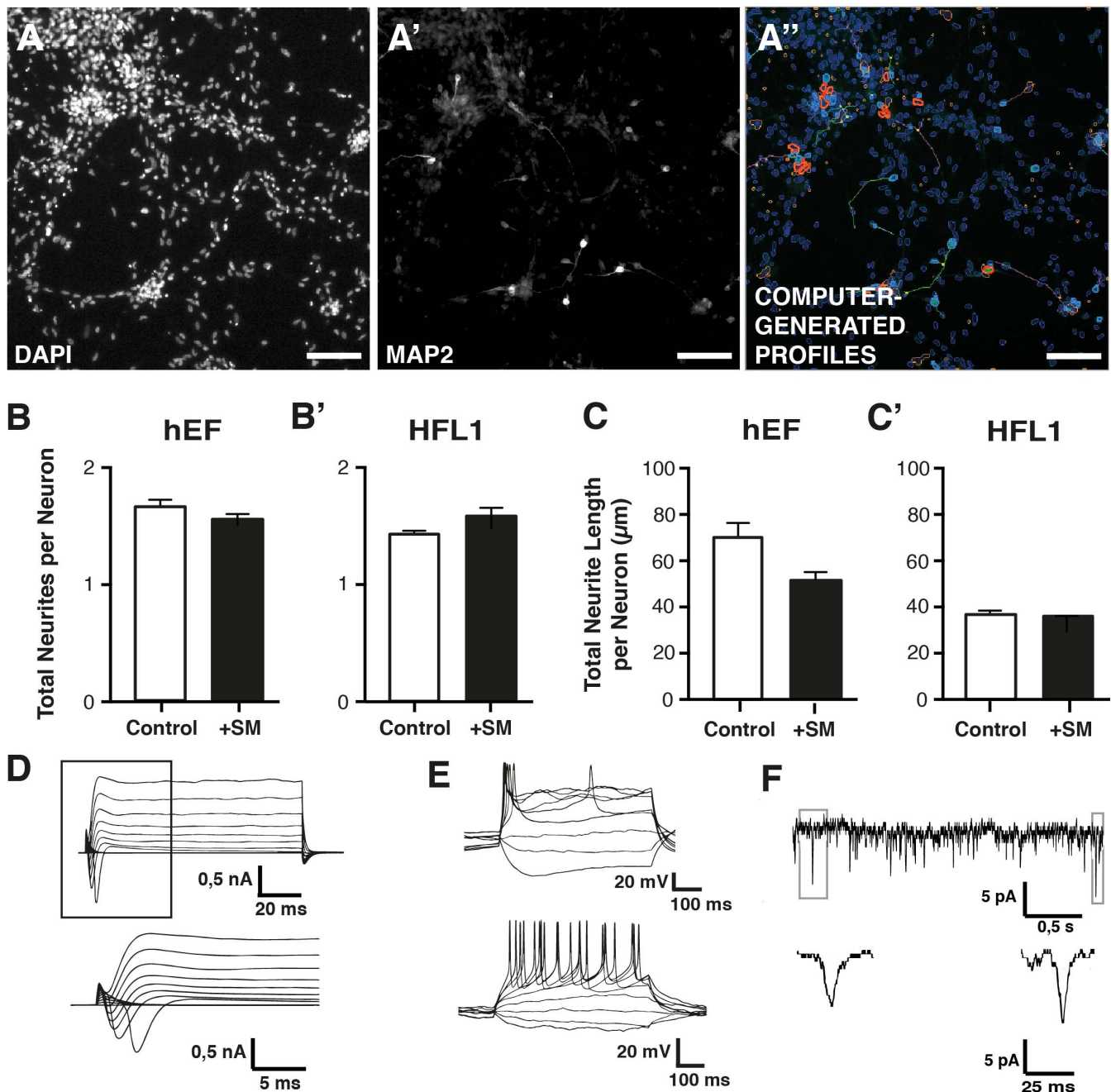


**Figure 3 | Assessment of the effect of small molecule treatment on morphology and electrophysiological properties of hiNs converted *in vitro*.**

(A, A' and A'') Images show how the Cellomics array scan “Neuronal Profiling” protocol is applied to each scanned image in the wells. After detection of DAPI<sup>+</sup> and MAP2<sup>+</sup> cells (A and A'), the program generates a profile designated with an individual color-coded mask in which a selection of different elements is performed (A''). Valid cell bodies – light blue; excluded cell bodies – red; valid nucleus – dark blue; excluded nucleus – orange; neurites (organized by size) – green and purple. (B and B') No difference was found in the total number of neurites per neuron, of MAP2<sup>+</sup> hiNs converted from hEFs and HFL1 with or without small molecules (n = 8). (C and C') Small molecule treatment had no effect on the total length of neurites per neuron (μm) in the MAP2<sup>+</sup> hiN cells converted from hEF or HFL1 cells (n = 8). (D, E and F) Electrophysiological properties of hiN *in vitro*. Representative traces of membrane sodium- and potassium currents following voltage depolarization steps ((D), full trace in upper panel the and a higher magnification in lower panel). Current-induced action potentials (AP) are shown in (E). Upper panel shows a response of few APs (recorded from n = 6 cells) and lower panel shows response of repetitive APs (recorded from n = 5 cells). hiNs show spontaneous synaptic activity 90 days post-conversion. A representative post-synaptic current at this stage is shown in (F). Scale bars: A, A' and A'' = 100 μm.

days *in vitro* after delayed transgene activation (Short); hiNs kept in culture for 4 days *in vitro* after delayed transgene activation and also treated with SMs (Short + SM); hiNs kept in culture for 9 days *in vitro* after delayed transgene activation (Long); hiNs kept in culture for 9 days *in vitro* after delayed transgene activation and also treated with SMs (Long + SM), and a control group of cells where transgenes

were delivered *in vitro* but not activated until after transplantation (Control). We have previously shown that such transduced, but not converted, fibroblasts can efficiently convert into neurons *in vivo* when transgenes are activated after transplantation via administration of doxycycline to the host, but that they remain as unconverted fibroblasts for up to 6 weeks if transgenes are not activated<sup>18</sup>.

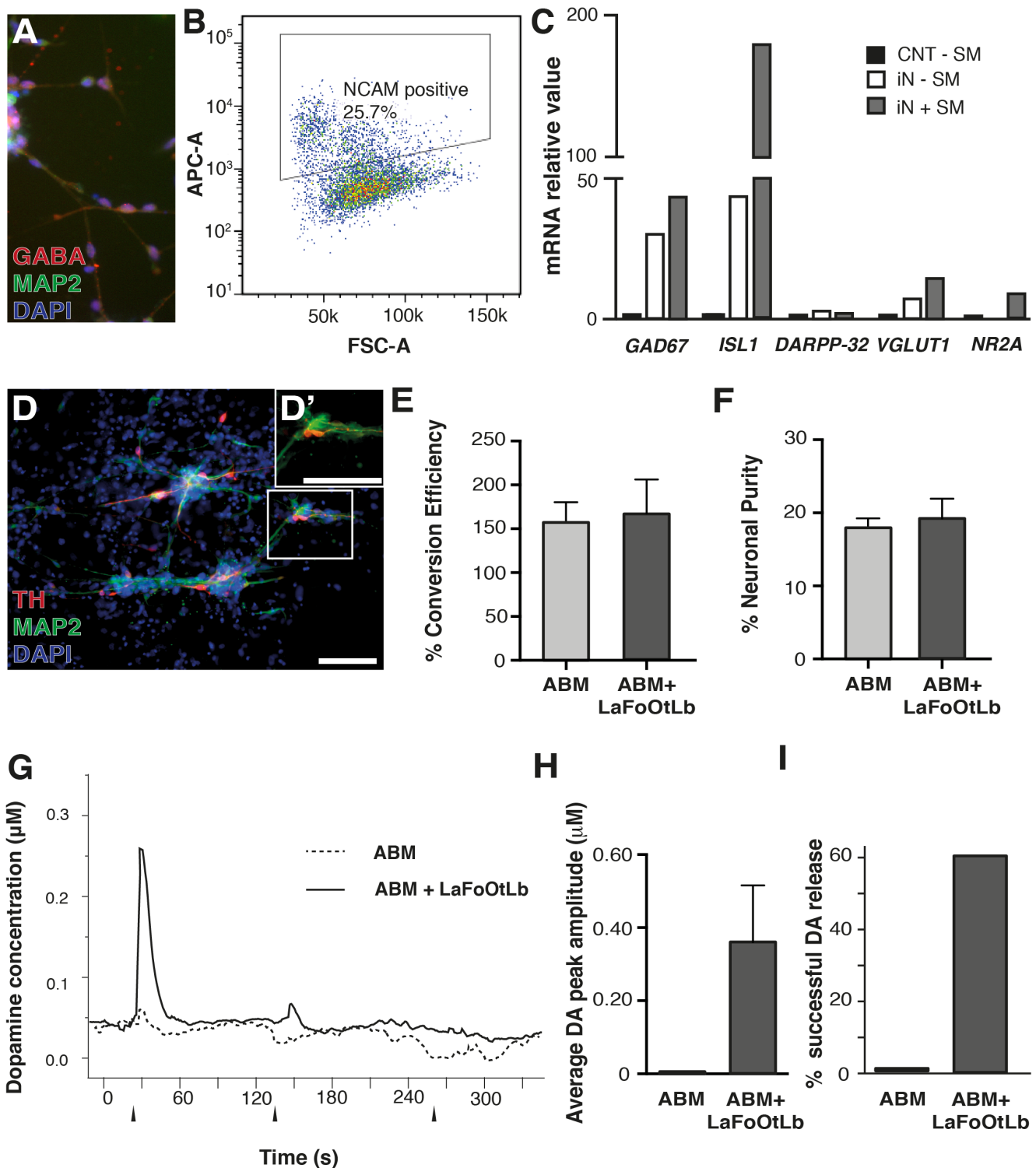


**Figure 4 | Study of the effect of small molecules and a new combination of conversion factors on neurotransmitter identity of the resultant hiNs.** (A) GABAergic neurons are present in hiN cultures obtained with delayed transgene activation and SM treatment. (B) Cloud plot resulting from the FACS-sorting of hNCAM<sup>+</sup> hiNs, obtained by transduction of HFL1 cells with ABM, using the Dox delay + SM protocol, 42 days after transgene activation. (C) Gene expression analysis (qPCR) of sorted hiNs 42 days after transgene activation, revealed the presence of high levels of the GABAergic genes *GAD67* and *ISL1* but low levels of *DARPP32*, along with the expression of the glutamatergic genes *VGLUT1*; results presented as mRNA relative value, normalized to an untreated fibroblast control and in relation to GAPDH housekeeping gene. (D and D') Fluorescence microscopy picture shows TH<sup>+</sup> hiNs, 15 days after transgene activation. (E and F) Conversion efficiency and neuronal purity, respectively, of hiNs converted from HFL1 cells, by using either ABM conversion factors or ABM and 4 DA determinants (ABM + LaFoOtLb), 12 days after transgene activation ( $n = 3$ ),  $p = n.s.$  (G) *In vitro* chronoamperometry recordings show release of dopamine upon KCl stimulation in cells converted with ABM and DA determinants (solid trace) but not in cells converted with ABM only (dashed trace). (H) The peak dopamine concentration in the recording buffer after the first KCl-induced release (I) After dopamine loading 60% of the KCl ejections resulted in detectable dopamine release in ABM+ DA determinants cells whereas no DA release event were detected in the ABM-only cells. Scale bars (D and D') = 100 μm.



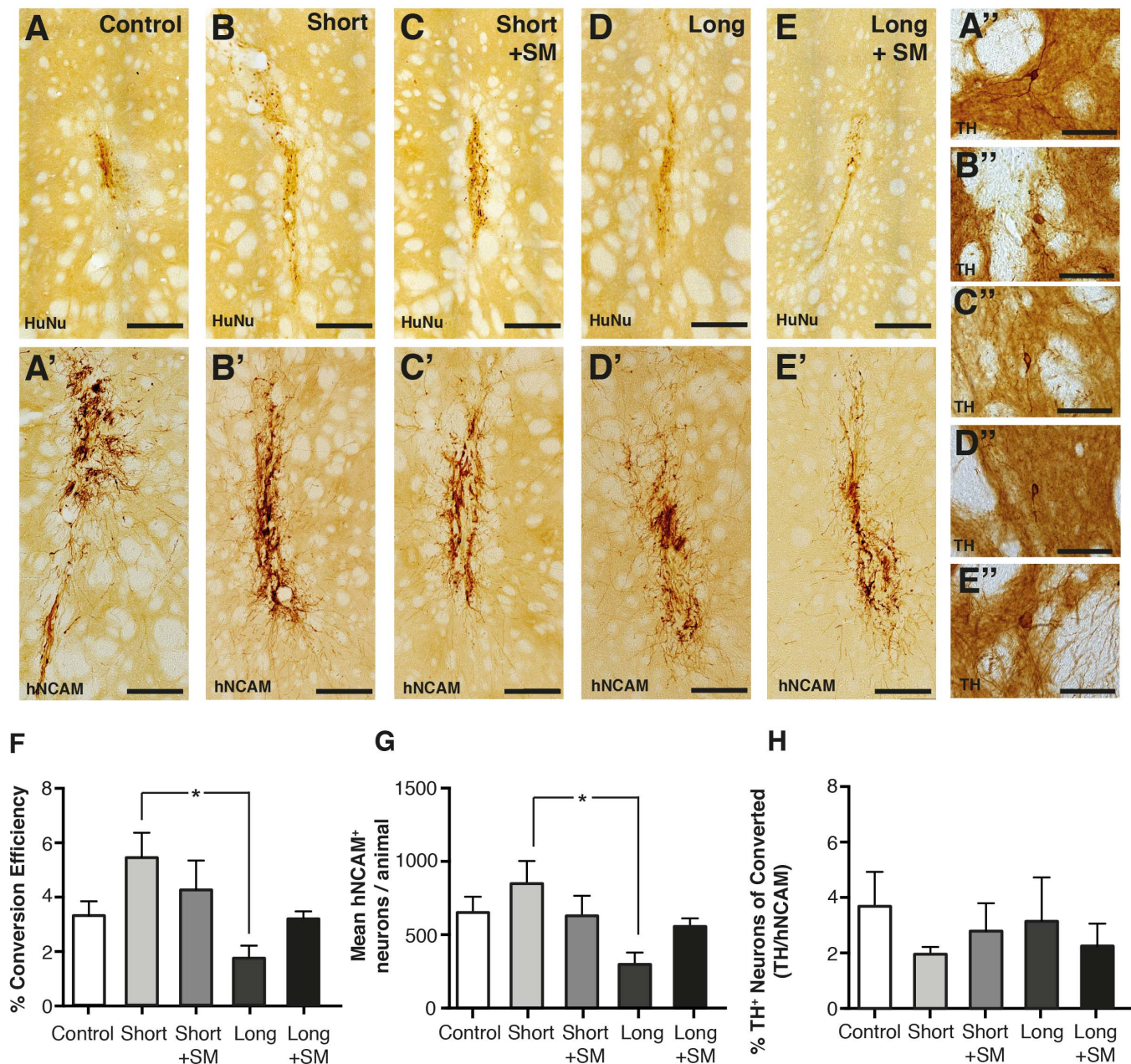


**Figure 5 | Comparison of neuronal conversion and generation of TH<sup>+</sup> neurons between experimental groups.** Grafts of hiNs detected using human nuclei (HuNu, A–E) are rich in neurons with a mature morphology (human-specific neural cell adhesion molecule; hNCAM) with significant axonal extension into the surrounding host striatum (A'–E'), (A) HFL1 cells transplanted and converted to hiNs *in vivo* (Control) (B) hiNs transplanted after dox delay and 4 days dox treatment *in vitro* (Short) (C) hiNs transplanted after dox delay, 4 days dox treatment and 2 days small molecule treatment *in vitro* (Short + SM) (D) hiNs converted after dox delay and 9 days dox treatment *in vitro* (Long) (E) hiNs converted after dox delay, 9 days dox treatment and 7 days of SMs *in vitro* (Long + SM); (A'', B'', C'', D'', E'') Depict TH<sup>+</sup> hiNs within the graft core. (F) Comparison of conversion efficiency of hiNs generated from all groups using a correction factor of an estimated 5% of cells surviving the transplantation procedure (n = 6), \* = p < 0.05, Long significantly lower compared to Short [Group,  $F_{(4,21)} = 3.53$ , p < 0.05, confirmed using a Tukey *post hoc*]; (G) Number of hNCAM<sup>+</sup> cells found, per animal, (n = 6), \* = p < 0.05, Long significantly lower compared to Short [Group,  $F_{(4,21)} = 3.36$ , p < 0.05, confirmed using a Tukey *post hoc*]; (H) Percentage of TH<sup>+</sup> cells of surviving hiN cells generated from all groups (n = 6), p = n.s. [Group,  $F_{(4,19)} = 0.36$ ]. Scale bars (A–E and A'–E') = 200  $\mu$ m; (A''–E'') = 100  $\mu$ m.

All animals were perfused and analysed 4 weeks after transplantation. Transplanted cells were selectively detected using an antibody that detects human nuclei (HuNu), which labels all human cells present in graft area (Fig. 5A, B, C, D, E), and another marker for human-specific neural cell adhesion molecule (hNCAM), which detects neurons of human origin (Fig. 5A', B', C', D', E'). Immunohistochemistry using these antibodies revealed that hiNs sourced from all culture conditions survived (Fig. 5A–E) and formed

neuron-rich grafts (Fig. 5A'–E') that spanned across >2 mm along the rostro-caudal axis.

The grafts had a similar appearance in all 5 groups (Fig. 5A'–E'). When further analysing the grafts with respect to time *in vitro* prior to transplantation (i.e. 4 vs 9 days in culture after transgene activation), we found no obvious effect on the survival of hiNs *in vivo* when looking at the grafts (Fig. 5B and D, and B', D'), but when quantifying the efficiency at which they generated neurons post transplanta-



tion, we found a small reduction in efficiency with longer time in culture before transplantation (Fig. 5F, G). Interestingly, while exposure to SMs *in vitro* significantly increases conversion efficiency and purity (Fig. 2A–C and<sup>14</sup>), exposure to SMs *in vitro* prior to transplantation did not result in a higher number of neurons after grafting (Fig. 5F, G). When assessing potential DA neurons in the grafts, we found that all conditions had a similar ability to generate TH<sup>+</sup> neurons, <4% (Fig. 5A''–E'', H).

Interestingly, this shows that addition of SMs do not have a positive effect on neuronal yield post transplantation. One explanation for this would be that the cells are not exposed to SMs for a sufficient amount of time *in vitro* prior to transplantation. To test this, we exposed the cells to SMs *in vitro* for the corresponding amount of time as in the *in vivo* experiment, removed the SMs and then let the cells convert *in vitro* (please see schematic in Supplementary Fig. S3A). We found that exposure to SMs for the same amount of time as the cells grafted lead to increased conversion efficiency (Supplementary Fig. S3B) and yield of TH-expressing neurons (Supplementary Fig. S3C).

## Discussion

We present a protocol for generation of functional and transplantable hiNs that is robust, efficient and reproducibly gives rise to a high proportion of functional hiNs *in vitro*. The protocol encompasses a delayed activation of transgene expression combined with delivery of small molecules that when combined, increases the purity and conversion efficiency of human fibroblasts.

As direct reprogramming converts one mature cell into another without a proliferative intermediate stage, the number of cells generated from any donor source is limited. Thus, increasing the number of output cells from a given number of input cells is very important in order to generate a sufficient number of cells for applications such as diagnostics, disease modelling and transplantation. In this study, we increase the number of hiNs obtained from a given number of fibroblasts by increasing the number of targeted cells and also by an optimal induction process of the targeted cells.

A recent publication has shown that addition of chemical compounds that inhibit SMAD signalling and activate canonical WNT signalling increase conversion efficiency and purity<sup>14</sup>. We found a cumulative effect of combining SMs with delayed activation of reprogramming genes. Our optimized protocol, with both delay of transgene activation and small molecules, increased the conversion efficiency 10-fold, and purity from less than 1% to 23%. This increased efficiency and purity should greatly facilitate using hiN conversion for disease modelling and experimental studies, and it alleviates the need for a selection step previously included in protocols with comparable high efficiencies<sup>14,17</sup>.

The hiNs obtained using our new protocol mature into functional neurons that display both inward and outward currents and with the ability to fire action potentials. In a previous study ABM alone was not found to be sufficient to generate functionally mature iNs that receive synaptic input<sup>15</sup>. However, here we could detect ABM-converted hiNs that receive synaptic input and displayed spontaneous activity after 90 days in co-culture with mouse astrocytes showing that if allowed enough time for maturation, the cells are able to send and receive synaptic input. When ABM is combined with DA fate determinants, functional DA neurons that take up and release DA can be obtained in high numbers using this protocol.

The possibility to obtain DA-iNs has previously been reported for mouse and human fibroblasts<sup>5,7,18,19</sup>, as well as via direct conversion of human pluripotent cells<sup>20</sup>. Mouse DA-iNs survive transplantation but little is known about the ability of human DA-hiNs to survive intracerebral transplantation into adult host brain<sup>19</sup>. Here, we present the first proof-of-principle experiments showing that hiNs survive and mature after transplantation into the adult rat brain. Cells

transplanted 4 and 9 days after initiation of iN conversion survived well and formed neuron-rich grafts 4 weeks after transplantation.

In these transplantation experiments we did not observe an effect of addition of SMs during conversion, as animals grafted with hiNs generated with doxycycline delay but no SMs survived equally well, formed grafts containing similar numbers of neurons and innervated the host brain to the same extent as hiNs generated in the presence of SMs. Thus, factors identified *in vitro* to enhance conversion do not necessarily translate to better *in vivo* performance of the cells, suggesting that additional factors present *in vitro* are lacking *in vivo*.

When analysing the grafts for potential dopaminergic neurons, we could detect TH-positive hiNs in all animals, albeit at lower frequency than previously reported for mouse cells<sup>19</sup>. Nevertheless, our data points towards the feasibility of developing such hiNs for cell replacement therapy applications. In this study we use hiNs obtained from fetal fibroblasts. Allografting of fetal ventral mesencephalic tissue as a dopaminergic replacement therapy in Parkinson's disease was developed and tested more than 20 years ago<sup>21,22</sup>. In these clinical trials, typically 3–5 embryos are used per brain hemisphere, and one of the main limiting factors for further development of cell replacement therapy for PD has been the low availability of human donor embryos<sup>21</sup>. Using iN technology, where fetal fibroblasts are collected, expanded and converted into DA neurons would greatly reduce the need for human embryos as one donated fetus could potentially provide a sufficient number of DA neurons to treat many patients<sup>23</sup>. In order to further assess the therapeutic potential of DA-hiNs and strategies for increasing TH neuron content in the grafts will need to be devised. Future studies should aim at investigating synaptic connections and functionality of the transplanted cells. To advance hiNs towards future cell replacement therapy also requires the development of new delivery systems that are non-integrative and where the transgenes are efficiently silenced or removed once neural conversion is complete, similar to what is being developed for induced pluripotent stem cells. In the future, iN conversion, like iPS reprogramming, also offers a unique opportunity for producing dopaminergic neurons for personalised cell replacement therapy using autologous cells.

## Methods

**Cells origin and culture procedures.** hEFs were obtained and expanded as previously described<sup>5</sup>. HFL1 (ATCC-CCL-153) cells were obtained from the American Type Culture Collection. For neural conversion *in vitro*, fibroblasts were plated in MEF medium at a density of 10 500 cells/cm<sup>2</sup> in 24-well plates (Nunc), previously coated with 0.1% gelatin or a combination of polyornithineP (15 µg/mL), fibronectin (0.5 mg/mL) and laminin (5 µg/mL). Before transplantation, cells were plated in MEF medium at a density of 50 000 cells/cm<sup>2</sup> in Petri dishes, previously coated with 0.1% gelatin.

**Viral vectors.** Doxycycline-regulated LVs expressing mouse cDNAs for ABM plus the TET-ON transactivator (FuW.rTA-SM2, Addgene) always co-transduced during conversion experiments, have been previously described<sup>3</sup>. LVs expressing mouse ORFs for Lmx1a, Lmx1b, Otx2, FoxA2 and Ngn2 were generated as previously described<sup>5</sup>.

**Generation of hiNs from human fibroblasts.** hEFs and HFL1 cells were transduced at a multiplicity of infection (MOI) of 5 (ABM, DA-determinants) and MOI of 10 (mrTA-FUW). Doxycycline (2 µg/mL) was added to the culture medium either 1, 3 or 5 days after transduction. Two days after transgene activation, MEF medium was replaced by neural differentiation medium (N2B27; Stem Cells). For small molecules (SMs) conditions (SM and Dox delay + SM), neural induction media was supplemented with growth factors at the following concentrations: 10 ng/mL BDNF, 2 ng/mL GDNF, 10 ng/mL NT3 (R&D Systems) and 0.5 mM db-cAMP (Sigma). The SMs CHIR99021 (Axon), SB431542, Noggin (R&D Systems) and LDN-193189 (Axon), were added to the media when stated in the text at the same concentrations as previously reported<sup>14</sup>. For the conditions Baseline and Dox delay, the neural induction media had different combinations of growth factors, namely 20 ng/mL BDNF, 10 ng/mL GDNF, 0.2 mM Ascorbic Acid and 100 nM Retinoic Acid. Every 2<sup>nd</sup>–3<sup>rd</sup> day, ¼ of the medium in wells was changed. Fixation was performed at the desired time points with paraformaldehyde 4%.

**qPCR analysis of FACS-sorted hNCAM<sup>+</sup> hiNs.** Human iNs were detached, spun down and resuspended in the staining buffer (HBSS supplemented with 45% BSA) for blocking (15 min @RT); hNCAM-APC antibody was added (1:50) and incubation





carried out for 15 minutes; A final centrifugation step and resuspension in HBSS 45% BSA, to which the secondary Nuclear orange antibody and DNase were added. The FACS-sorted samples were used for qPCR analysis, carried out using SYBR Green as described previously<sup>5</sup>. All primers were validated on subdissected human tissue before use.

**Transplantations.** 30 Adult female Sprague Dawley rats (225–250 g) were used as graft recipients in these experiments and were housed on a 12 h light/dark cycle with *ad libitum* access to food and water. All procedures were conducted in accordance with guidelines set by the Ethical Committee for the use of laboratory animals at Lund University.

All surgical procedures were conducted as described in detail in<sup>24</sup>. Animals were immunosuppressed using a dose of 10 mg/kg of ciclosporin A injected i.p. daily. Doxycycline treatment was maintained *in vivo* by administration p.o. via the drinking water (1 mg/ml). Animals were pre-treated for one week prior to transplantation and then maintained for the duration of the experiment at a dose of 100 mg/kg. For transplantation a total of 400,000 cells were transplanted into the striatum of each animal at a concentration of 100,000 cells/ $\mu$ l.

**Immunostaining, imaging and *in vitro* quantifications.** Immunohistochemical procedures were performed as has previously been described in<sup>25</sup>. For *in vitro* experiments, the total number of DAPI<sup>+</sup> and MAP2<sup>+</sup> cells per well was quantified using the Cellomics Array Scan (Array Scan VTI, Thermo Fischer). Applying the program “Target Activation”, 30–50 fields (10 $\times$  magnification) were acquired, in a spiral fashion, from center to outside. The same array was set to perform the analysis of number and length of neurites present in the wells, by using the program “Neuronal Profiling”. Conversion efficiency was calculated as defined in<sup>3</sup> and neuronal purity was calculated as described in<sup>14</sup>. The number of GABA<sup>+</sup> and TH<sup>+</sup> neurons was obtained manually by counting all GABA<sup>+</sup>/MAP2<sup>+</sup> or TH<sup>+</sup>/MAP2<sup>+</sup> double-positive cells with a neuronal morphology in 36 randomly acquired fields (20 $\times$  magnification), per well.

**Electrophysiology.** Patch-clamp electrophysiology was performed on hiN at day 48–50 and day 90 post-conversion. Cultured hiNs, with or without glia at day 50 and with glia at day 90, were grown on coverslips and transferred to a recording chamber and submerged in a continuously flowing Krebs solution gassed with 95% O<sub>2</sub> - 5% CO<sub>2</sub> at 28°C. The composition of the standard solution was (in mM): 119 NaCl, 2.5 KCl, 1.3 MgSO<sub>4</sub>, 2.5 CaCl<sub>2</sub>, 25 Glucose and 26 NaHCO<sub>3</sub>.

Recordings were made with a Multiclamp 700B amplifier (Molecular Devices), using borosilicate glass pipettes (3–7 MOhm) filled with the following intracellular solution (in mM): 122.5 potassium gluconate, 12.5 KCl, 0.2 EGTA, 10 Hepes, 2 MgATP, 0.3 Na<sub>3</sub>GTP and 8 NaCl adjusted to pH 7.3 with KOH. Data were acquired with pClamp 10.2 (Molecular Devices); current was filtered at 0.1 kHz and digitized at 2 kHz.

Cells with neuronal morphology with round cell body were selected for whole-cell patch clamp. Resting membrane potentials were monitored immediately after breaking-in in current-clamp mode. Thereafter, cells were kept at a membrane potential of –60 mV to –80 mV, and 500 ms currents were injected from –20 pA to +90 pA with 10 pA increments to induce action potentials. For sodium and potassium current measurements cells were clamped at –70 mV and voltage-depolarizing steps were delivered for 100 ms at 10 mV increments.

**Amperometric measurements of DA release.** The cells attached to a glass coverslip were placed in a custom-made flow chamber (volume 0.4 ml, flow rate 0.7 ml/min, temperature kept at 37°C). During the recordings PBS lite with 100 mg/L magnesium and 100 mg/L calcium (pH 7.4) was allowed to flow over the coverslip. The electrode was placed immediately downstream of the cultured cells so that any dopamine release by the cells would be detected in the flowing buffer. Simultaneously with a digital marking signal 100  $\mu$ l of 120 mM KCl was added to the flow of buffer upstream of the cells in order to depolarize the cells and induce release of synaptic vesicles. High speed chronoamperometric recordings were made using FAST-16mkII hardware and software (Quanteon, L.L.C. Nicholasville, KY, USA) fitted with carbon fiber electrodes (fiber diameter 30  $\mu$ m; exposed length 120–150  $\mu$ m, type SPF1a, Quanteon, L.L.C. Nicholasville, KY, USA). Electrodes were dip coated in nafion and dried in 200°C for 5 minutes as previously described<sup>26</sup>. Each electrode was individually calibrated for linearity of response to increments of dopamine (3  $\times$  2 mM dopamine) and for selectivity of dopamine over ascorbic acid. The linearity of the response to dopamine was confirmed in all electrodes with a r<sup>2</sup> constant of >0.999 and the selectivity versus ascorbic acid was determined to >2000:1 for all electrodes. The limit of detection, defined as 3 standard deviations from baseline, was <21 nM dopamine. A square wave current was applied (+0.55 V–0 V) against an Ag/AgCl reference electrode that was incorporated into the recording chamber and 80% of the signal was recorded to determine the oxidation and reduction current. Recordings were made at 2 Hz where each datapoint represents the average of 5 square wave cycles. The current arising from the induced oxidation/reduction of dopamine is proportional to the concentration of dopamine in the solution. To pre-load the cells with exogenous dopamine, a separate supply of buffer containing dopamine was connected to the tubing that supplied the PBS lite to the recording chamber. The concentration of dopamine in the buffer was 10–15  $\mu$ M as measured by the electrochemical carbon fiber electrode. The dopamine flow was terminated after 60 s and 120 seconds later, when the signal had stabilized at baseline, a short pulse of

100  $\mu$ l, 120 mM KCl was added directly to the solution in the recording chamber. 3 consecutive KCl applications were made after each DA loading session.

It is known from previous studies *in vivo* that the amplitude of the KCl-induced dopamine release is reduced with rapid repeated depolarizations<sup>25</sup>. Perturbations caused by the addition of KCl to the recording buffer in this setup can cause a minor signal disturbance. In order to verify that the signal recorded in these recordings were genuine dopamine release events and not noise produced by liquid perturbations or other possible sources of environmental noise, strict criteria were used to categorize release events as genuine release events. These criteria were: 1) amplitude should be at least 3 times the limit of detection (here 63 nM), 2) the amplitude of the 2<sup>nd</sup> and 3<sup>rd</sup> KCl evoked release should be lower than the first release.

All data was analysed using FAST analysis version 4.0 for Mac (quanteon LLC, Lexington, KY, USA). Peak amplitude was calculated as the maximum dopamine concentration after KCl ejection minus the baseline prior to KCl injection.

***In vivo* quantifications.** The total number of surviving human cells [human nuclei (HuNu<sup>+</sup>)], human neurons (hNCAM<sup>+</sup>) and TH<sup>+</sup> cells were estimated in a series of every eighth coronal section of each animal. Cell counting and conversion efficiency calculation was performed as described previously<sup>18</sup>. Percentage of TH<sup>+</sup> neurons of converted was calculated as the percentage of TH<sup>+</sup> cells, out of hNCAM<sup>+</sup> neurons. All quantifications were performed in blind.

**Statistical analysis.** All data are expressed as mean  $\pm$  the standard error of the mean. All statistical analyses were conducted using the GraphPad Prism 6.0c. An alpha level of  $p < 0.05$  was set for significance.

Conversion efficiency (both *in vitro* and *in vivo*), neuronal purity, reduction in cell number and percentage of TH<sup>+</sup> neurons of converted neurons were compared using a one-way ANOVA with a Tukey post hoc. A two-tailed Student's t-test was used to compare the effects of SM in Figures 3, 4.

- Chambers, S. M. & Studer, L. Cell fate plug and play: direct reprogramming and induced pluripotency. *Cell* **145**, 827–830, DOI:S0092-8674(11)00597-6 (2011).
- Takahashi, K. & Yamanaka, S. Induction of pluripotent stem cells from mouse embryonic and adult fibroblast cultures by defined factors. *Cell* **126**, 663–676, DOI:S0092-8674(06)00976-7 (2006).
- Vierbuchen, T. *et al.* Direct conversion of fibroblasts to functional neurons by defined factors. *Nature* **463**, 1035–1041, DOI:nature08797 (2010).
- Lujan, E., Chanda, S., Ahlenius, H., Sudhof, T. C. & Wernig, M. Direct conversion of mouse fibroblasts to self-renewing, tripotent neural precursor cells. *Proc Natl Acad Sci U S A* **109**, 2527–2532, DOI:10.1073/pnas.1121003109 (2012).
- Pfisterer, U. *et al.* Direct conversion of human fibroblasts to dopaminergic neurons. *Proc Natl Acad Sci U S A* **108**, 10343–10348, DOI:1105135108 (2011).
- Son, E. Y. *et al.* Conversion of mouse and human fibroblasts into functional spinal motor neurons. *Cell Stem Cell* **9**, 205–218, DOI:S1934-5909(11)00377-8 (2011).
- Caiazzo, M. *et al.* Direct generation of functional dopaminergic neurons from mouse and human fibroblasts. *Nature* **476**, 224–227, DOI:nature10284 (2011).
- Liu, M. L. *et al.* Small molecules enable neurogenin 2 to efficiently convert human fibroblasts into cholinergic neurons. *Nat Commun* **4**, 2183, DOI:10.1038/ncomms3183 (2013).
- Iovino, M. *et al.* The novel MAPT mutation K298E: mechanisms of mutant tau toxicity, brain pathology and tau expression in induced fibroblast-derived neurons. *Acta Neuropathol* **127**, 283–295, DOI:10.1007/s00401-013-1219-1 (2014).
- Chanda, S., Marro, S., Wernig, M. & Sudhof, T. C. Neurons generated by direct conversion of fibroblasts reproduce synaptic phenotype caused by autism-associated neuroigin-3 mutation. *Proc Natl Acad Sci U S A* **110**, 16622–16627, DOI:10.1073/pnas.1316240110 (2013).
- Marro, S. *et al.* Direct lineage conversion of terminally differentiated hepatocytes to functional neurons. *Cell Stem Cell* **9**, 374–382, DOI:10.1016/j.stem.2011.09.002 (2011).
- Ali, F., Stott, S. R. & Barker, R. A. Stem cells and the treatment of Parkinson's disease. *Exp Neurol*, DOI:10.1016/j.expneurol.2012.12.017 (2013).
- Takahashi, K. & Yamanaka, S. Induced pluripotent stem cells in medicine and biology. *Development* **140**, 2457–2461, DOI:10.1242/dev.092551 (2013).
- Ladewig, J. *et al.* Small molecules enable highly efficient neuronal conversion of human fibroblasts. *Nat Methods* **9**, 575–578, DOI:10.1038/nmeth.1972 (2012).
- Pang, Z. P. *et al.* Induction of human neuronal cells by defined transcription factors. *Nature* **476**, 220–223, DOI:nature10202 (2011).
- Yoo, A. S. *et al.* MicroRNA-mediated conversion of human fibroblasts to neurons. *Nature* **476**, 228–231, DOI:10.1038/nature10323 (2011).
- Zhang, Y. *et al.* Rapid single-step induction of functional neurons from human pluripotent stem cells. *Neuron* **78**, 785–798, DOI:10.1016/j.neuron.2013.05.029 (2013).
- Torper, O. *et al.* Generation of induced neurons via direct conversion *in vivo*. *Proc Natl Acad Sci U S A* **110**, 7038–7043, DOI:10.1073/pnas.1303829110 (2013).
- Kim, J. *et al.* Functional Integration of Dopaminergic Neurons Directly Converted from Mouse Fibroblasts. *Cell Stem Cell*, DOI:S1934-5909(11)00442-5 (2011).
- Theka, I. *et al.* Rapid generation of functional dopaminergic neurons from human induced pluripotent stem cells through a single-step procedure using cell lineage transcription factors. *Stem Cells Transl Med* **2**, 473–479, DOI:10.5966/sctm.2012-0133 (2013).





21. Barker, R. A., Barrett, J., Mason, S. L. & Bjorklund, A. Fetal dopaminergic transplantation trials and the future of neural grafting in Parkinson's disease. *Lancet Neurol* **12**, 84–91, DOI:10.1016/S1474-4422(12)70295-8 (2013).
22. Lindvall, O. *et al.* Grafts of fetal dopamine neurons survive and improve motor function in Parkinson's disease. *Science* **247**, 574–577 (1990).
23. Pfisterer, U. *et al.* Efficient induction of functional neurons from adult human fibroblasts. *Cell Cycle* **10**, 3311–3316, doi:17584 (2011).
24. Grealish, S. *et al.* The A9 dopamine neuron component in grafts of ventral mesencephalon is an important determinant for recovery of motor function in a rat model of Parkinson's disease. *Brain* **133**, 482–495, DOI:10.1093/brain/awp328 (2010).
25. Lundblad, M. *et al.* Chronic intermittent L-DOPA treatment induces changes in dopamine release. *J Neurochem* **108**, 998–1008, DOI:10.1111/j.1471-4159.2008.05848.x (2009).
26. Gerhardt, G. A., Oke, A. F., Nagy, G., Moghaddam, B. & Adams, R. N. Nafion-coated electrodes with high selectivity for CNS electrochemistry. *Brain Res* **290**, 390–395 (1984).

## Acknowledgments

We thank Ingar Nilsson, Christina Isaksson Ulla Jarl, and Michael Sparrenius for technical assistance. This study was supported by grants from the European Community's 7th Framework Programme through NeuroStemcellRepair 602278, The Swedish Research Council (K2012-99X-22324-01-5 and K2014-61X-20391-08-4), Bagadilico (70862601), MultiPark – A Strategic Research Area at Lund University and Swedish Parkinson Foundation. The research leading to these results has received funding from the European

Research Council under the European Union's Seventh Framework Programme (FP/2007–2013)/ERC Grant Agreement n. 309712.

## Author contributions

M.Pe., U.P., O.T. and S.L. planned, conducted and analysed experiments. D.R. performed electrophysiology experiments, M.L. performed amperometry experiments. M.Pe. and S.G. planned, conducted and analyzed transplantation experiments. M.Pa. conceived study, analysed data and wrote manuscript. S.G. and M.Pe. co-wrote the manuscript and prepared final figures. All authors reviewed and gave input to the manuscript

## Additional information

**Supplementary information** accompanies this paper at <http://www.nature.com/scientificreports>

**Competing financial interests:** The authors declare no competing financial interests.

**How to cite this article:** Pereira, M. *et al.* Highly efficient generation of induced neurons from human fibroblasts that survive transplantation into the adult rat brain. *Sci. Rep.* **4**, 6330; DOI:10.1038/srep06330 (2014).



This work is licensed under a Creative Commons Attribution-NonCommercial-NoDerivs 4.0 International License. The images or other third party material in this article are included in the article's Creative Commons license, unless indicated otherwise in the credit line; if the material is not included under the Creative Commons license, users will need to obtain permission from the license holder in order to reproduce the material. To view a copy of this license, visit <http://creativecommons.org/licenses/by-nc-nd/4.0/>